Hindawi
Advances in Materials Science and Engineering
Volume 2018, Article ID 8082368, 14 pages
https://doi.org/10.1155/2018/8082368

Research Article

Design and Climate-Responsiveness Performance Evaluation of an Integrated Envelope for Modular Prefabricated Buildings

Junjie Li,[1] **Shuai Lu**,[2] **Wanlin Wang**,[1] **Jie Huang**,[1] **Xinxing Chen**,[1] **and Jiayi Wang**[1]

[1]*School of Architecture and Design, Beijing Jiaotong University, Beijing 100044, China*
[2]*School of Architecture and Urban Planning, Shenzhen University, Shenzhen 518060, China*

Correspondence should be addressed to Shuai Lu; lyushuai@szu.edu.cn

Received 26 February 2018; Accepted 5 May 2018; Published 7 August 2018

Academic Editor: Abílio De Jesus

Copyright © 2018 Junjie Li et al. This is an open access article distributed under the Creative Commons Attribution License, which permits unrestricted use, distribution, and reproduction in any medium, provided the original work is properly cited.

Modular prefabricated buildings effectively improve the efficiency and quality of building design and construction and represent an important trend in the development of building industrialization. However, there are still many deficiencies in the design and technology of existing systems, especially in terms of the integration of architectural performance defects that cannot respond to occupants' comfort, flexibility, and energy-saving requirements throughout the building's life cycle. This research takes modular prefabricated steel structural systems as its research object and sets the detailed design of an integrated modular envelope system as the core content. First, the researcher chose two types of thermal insulation materials, high insulation panels and aerogel blankets, in order to study the construction details of integrated building envelopes for modular prefabricated buildings. Focusing on the weakest heat point, the thermal bridge at the modular connection point, this work used construction design and research to build an experimental building and full-scale model; the goal was to explore and verify the feasibility of the climate-responsive construction technique called "reverse install." Second, as a response to climate change, building facades were dynamically adjusted by employing different modular building envelope units such as sunshades, preheaters, ventilation, air filtration, pest control, and other functional requirements in order to improve the building's climate adaptability. Finally, based on the above structural design and research, this study verified the actual measurements and simulation, as well as the sustainability performance of the structure during the operational phase, and provided feedback on the design. The results highlight the environmental performance of each construction detail and optimized possibilities for an integrated envelope design for modular prefabricated buildings during both the design and renovation phases.

1. Introduction

1.1. Research Background. The energy and environmental crisis of the 1970s gave birth to a global awareness of and widespread attention to the issue of sustainable development [1]. In this context, the field of architecture has also expanded, and sustainable architecture has become an important and rapidly developing research proposition [2]. Owing to the environment's potential for sustainability, society's needs, and certain economic aspects (such as saving construction time, improving building quality, reducing material waste, alleviating environmental loads, and reducing cost) [3–5], prefabricated buildings have become an important research topic in sustainable architecture, now playing an essential role in Western urban construction [6, 7].

Modularization is one means of operation in the manufacture of industrial products. Its production efficiency and delicacy are well established in production [8, 9]. If we look at the problem of building industrialization with an eye towards product manufacture, modular design, and the overall construction methodology, most components are prefabricated at the factory and assembled on-site. In such cases, building space is integrated, construction time is minimized, and on-site construction errors are reduced (as shown in Figure 1) [10, 11]. Modular design also embodies the concept of sustainable development and "green" construction. However,

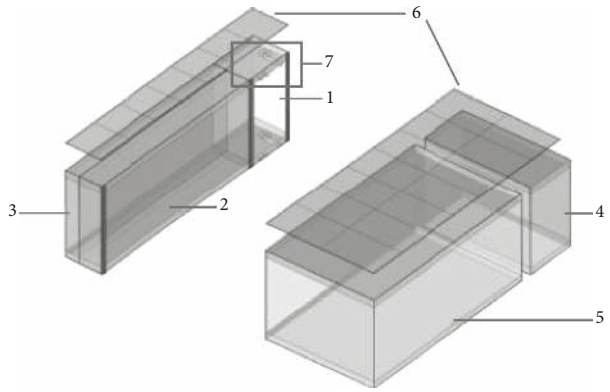

Figure 1: Modular prefabricated building prototype (source: authors' own data).

Figure 2: Hoisting and installation of a modular prefabricated building prototype (source: authors' own data).

there are currently many deficiencies in both the design and certain technical aspects of the existing system [12], especially with regard to defects in architectural performance and integrated design (as shown in Figure 2). Currently, they cannot respond to occupants' requirements for comfort, flexibility, and energy-saving throughout the building's life cycle [13].

The form of the building envelope has a decisive influence on building performance during the operating phase; it is also one of the most important elements of modular prefabricated buildings [14]. Therefore, this research focused on the sustainability-related performance of modular prefabricated buildings, mainly exploring the construction details of integrated building envelopes and their climate responsiveness.

A master of modernist architecture Le Corbusier first proposed the idea of a "drawer-type residence" in 1947. This served to introduce the topic of modularization and standardization in building design (as shown in Figure 3) [15]. In the 1960s, a Dutch scholar named Habraken proposed the notion of open architecture, creating the SI housing system for residential architecture [16]. The effective separation of S (the skeleton) and I (the infill) led to houses that offered structural durability, flexibility in the indoor space, and quality filling [17]. The German and American architects, Konard Wachsmann and Walter Gropius, respectively, jointly developed the assembly-type General Panel System in 1945. According to the modules, these buildings were decomposed into composite panels, thermal insulation, inside and outside walls, floors, ceiling, roofs, and so on. These architects also developed

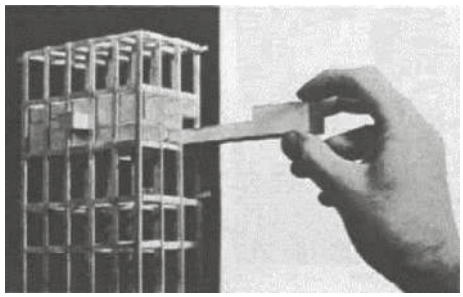

Figure 3: Le Corbusier: drawer-type residence (source: [15]).

a connection node system between the plates to meet the requirements of rapid development and system expansion [18, 19]. Ochs invented a prefabricated timber structural envelope module to integrate active equipment such as microheat pumps and full heat exchangers into single building components [20]. The design not only saved time and labor during the construction phase but also satisfied the energy-saving and thermal comfort aspects of building performance [21].

1.2. Objective of This Study. This research focused on the construction details, design, and effective evaluation of integrated building envelopes for modular prefabricated buildings. Three goals were pursued: (1) to use a rational integrated building envelope design to improve the physical environment and energy-saving performance during a modular prefabricated building's operational phase, (2) to resolve weaknesses related to thermal bridges at the connection points of modular prefabricated buildings and advance their sustainable performance during the operational phase, and (3) to improve the climate adaptability capacity of the overall building environment by optimizing the design of integrated building envelopes.

2. Methodology

This research examined modular prefabricated buildings with steel structural systems and set the details of an integrated module design for an envelope system as the core content. Buildings with steel structures offer advantages during prefabrication, transportation, modular hoisting, and installation and thus are the preferred structural system in prefabricated architecture [22]. However, compared with PC and wooden structural systems, the heat transferability of steel structures is stronger and faster, obvious disadvantages in terms of thermal insulation performance [23]. Therefore, this research chose two types of thermal insulation materials, high insulation panels (HIPs) and aerogel blankets (ABs), to study the construction details of integrated building envelopes for modular prefabricated buildings. Focusing on the weakest heat points, the thermal bridges at modular connection points, this study employed construction detail design and research to build an experimental building and full-scale building model. The goal was to explore and verify the feasibility of the climate-responsive construction detail technique called "reverse install." Moreover, the envelope's structural component system featured modularization,

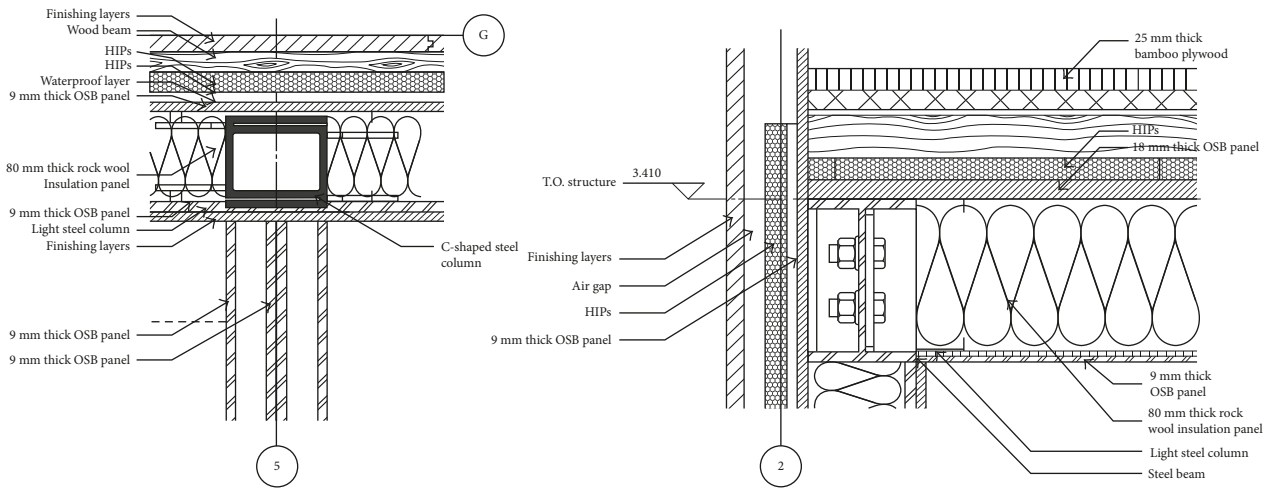

Figure 4: Exterior wall construction detail using the HIP's insulation layer (source: authors' own data).

standardization, and prefabrication [24], characteristics that can be optimized for climate responsiveness. To accommodate new needs stemming from climate change, building facades were dynamically adjusted by using different modular building envelope units, including sunshades, preheaters, ventilation, air filtration, pest control, and other functional requirements. The goal was to improve the building's performance related to climate adaptability. Based on the above structural design and research, this study verified the actual measurements and simulation, as well as the sustainability performance of the construction during the operational phase, and provided design feedback.

2.1. The Reverse Install Integrated Building Insulation Envelope Technique

2.1.1. Using HIPs to Improve Heat Preservation and Solve the Thermal Bridge Problem. Research on ultra-thin vacuum insulation panels began in Europe in 1972. At first, this type of insulation was primarily used for heat preservation in transportation equipment, sophisticated cold storage machinery, and so on. As the research developed, the panels were increasingly applied in the field of architecture, to floors, doors and windows, roofs, interior walls, and building exteriors [25]. HIPs are composed of two parts: a high barrier composite film and the core material. The high barrier composite membrane comprised inorganic fiber cloth, a multilayer aluminum foil, and a multilayer compact material that protects and affixes the HIPs. The high-quality barrier diaphragm guarantees the service life. The core material is made up of porous inorganic substances such as nanometer-superfine silica. The porous structure of the vacuum is beneficial in facilitating low thermal conductivity [26].

The wall construction details for the building used in this research, from inside to outside, were as follows: the interior panel was a 9 mm thick OSB panel that served as a structural layer. There was also a light steel structural infill with an 80 mm thick rock wool insulation panel.

Figure 5: Building's exterior wall with HIPs employed during the building process (source: authors' own data).

There was another 18 mm thick OSB panel that also served as a structural layer, and a waterproof layer composed of a 15 mm thick double-layer HIP with a wood keel and an air gap exterior panel [27], as shown in Figure 4. The building used a 300 mm module, which included the axis, size of the openable doors and windows, and vertical dimensions of the building. Therefore, the HIP dimensions were also controlled according to the following four types: 300 mm × 300 mm, 300 mm × 600 mm, 300 mm × 400 mm, and 400 mm × 600 mm (as shown in Figure 5).

Different from the other ordinary aspects of envelope construction, modular connections must be installed after the module is transported to the site. Installation relies on an integrated envelope panel to improve construction efficiency. Therefore, an integrated envelope unit must first be constructed in a factory, according to the following steps: the OSB panel is used as the basement material, and the HIP's insulation layer is attached to the OSB, with the keel frame in between. It is then covered with a layer of finishing material, while the other side of the OSB is covered with a waterproof layer. Then, the integrated envelope units (including the structural, insulation, moisture-proofing, and finishing layers) are installed entirely as a hanging board at the module's connection point (as shown in Figure 6).

Figure 6: Reverse install integrated building insulation envelope technique (source: authors' own data).

2.1.2. Using ABs to Improve Heat Preservation and Solve the Thermal Bridge Problem

(1) Integrated Building Envelope Using ABs. In 1931, the American researcher S. Kistler developed silica aerogels via an ethanol-based supercritical drying technique. In the 1970s and 1980s, aerogel was used in Cherenkov detectors and to store rocket fuel. In the 1990s, the material was employed as heat insulation for the space shuttle and in US jet propulsion laboratories [28]. In architecture, aerogel is of interest because of the microvoid nanometer-restrained heat transfer of air molecules. Also, the refractive index of silica aerogel is close to 1, and the ratio of the extinction coefficient to infrared and visible light is more than 100; the result is the effective pass-through of sunlight, preventing infrared radiation and related increases in ambient temperature. Therefore, aerogels have become an ideal transparent insulation material, applied in both solar energy utilization and building energy conservation [29]. By means of synthetic methods, aerogel can be combined with glass fiber cotton or preoxidized fiber felt. AB's thermal conductivity can be as low as 0.015 W/(m·K) at a normal temperature and atmospheric pressure. Compared with traditional materials, the thermal conductivity of AB is three to five times better than rock wool of the same thickness [30]. In addition, AB offers certain advantages such as A1 fire protection; it is also easy to cut, lightweight, and has a high hydrophobicity and thus is the insulation material most suitable for prefabricated buildings (as shown in Figure 7).

The construction details of the building envelope using AB as insulation were as follows: a 15 mm thick OSB panel was used as the basement material, and a 10 mm thick AB was attached to the OSB structural layer. The other side of the OSB was attached with a waterproof layer, an upper layer covered with keel, and an exterior finishing layer (as shown in Figures 8 and 9). Since the AB layer had no size constraints, the size of the thermal insulation material could be adjusted according to the modular building's modules.

(2) Design for Thermal Bridge Prevention at Module Connection Points. When the four corners of a module are supported by steel columns and double-steel columns are used at the connection points of a building module, the two modules must be spliced. In the absence of a well-designed thermal insulation, the steel columns may be directly exposed to the outside on the integrated external wall. This can lead to weaknesses in the thermal bridge to the building environment. A detailed construction plan designed to avoid this weakness must be based on the basic modules of the building and an integrated building envelope unit; after the two building modules are assembled on-site, these modules will hang on the construction. In this case study, the integrated building envelope unit was 600 mm at the two building modules' connection points, as determined by the experimental building's module size. The specific process used a reverse install technique to attach the AB, waterproof layer, keel, and exterior finishing layer to the OSB structural layer. After the integrated envelope unit was constructed, it was installed with the reserved connecting piece of the main steel beam structure and fastened with self-tapping nails. This method integrated the structural, thermal insulation, moisture-proofing, and exterior finishing layers into a single unit, which will be beneficial in the multiple assemblies and disassemblies that often accompany prefabricated buildings (as shown in Figures 10 and 11).

2.2. Replaceable Modules Based on Climate Adaptation. There are two kinds of climate regulation characteristics related to building envelopes and the spaces they form: climate defense and climate utilization. Climate defense reflects the "buffer" strategy of auxiliary functional space, while climate utilization refers to the dynamic regulation of the joint actions of the building's envelope and space. Thomas Herzog believed that architecture's form can be conceptualized as similar to human skin, and the internal function can be understood like bones. The clothing people wear, its different styles and materials, expresses human diversity and societal individuality. Clothing and building envelopes are similar in that they are both public and private "interfaces" [32]. A building's envelope contains a variety of mass flows and therefore requires multiple functions [33]. According to the time, climate, status of use, and other factors, a building skin incorporates a combination of functions, some complementary and some in competition with one another, including sight penetration, sight view, natural lighting, shading, heat preservation, heating, ventilation, air filtration, natural risk barriers, sound insulation, and climatic buffers.

The southern-facing outer layer of a building's double-skin facade (DSF) was designed and studied in this research. Various replaceable modular designs based on climate adaptation and occupants' requirements were imparted to the outer interface [34, 35]. In the southern facade's vertical direction, the outer interface of the DSF was divided into three segments from bottom to top (according to the human scale and occupant requirements); these included the protected, sight, and shading zones (as shown in Figure 12). The aluminum material panel provided the possibility of numerically controlling the machined processing of the outer layer. Through a computer parameterization algorithm, the bottom of the facade's outer layer (called the protected zone) was designed to be the smallest aperture; this was to guarantee the sturdiness and compactness of the

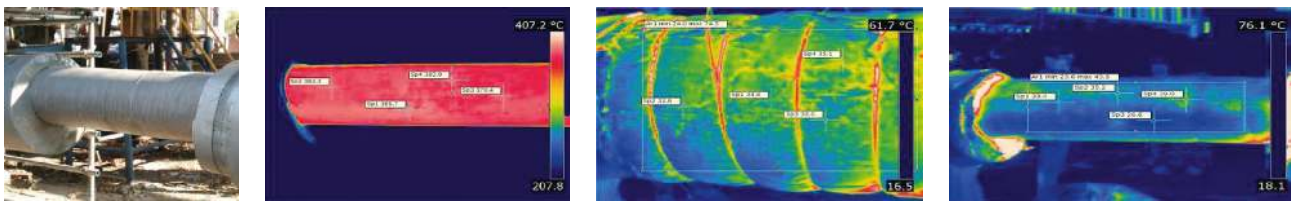

(a) (b) (c) (d)

Figure 7: Contrast of infrared imaging with the rock wool panel and AB as insulation materials (source: [31]). (a) Pipe photo, (b) infrared thermal imaging of the pipe, (c) rock wool panel as the insulation layer, and (d) AB as the insulation layer.

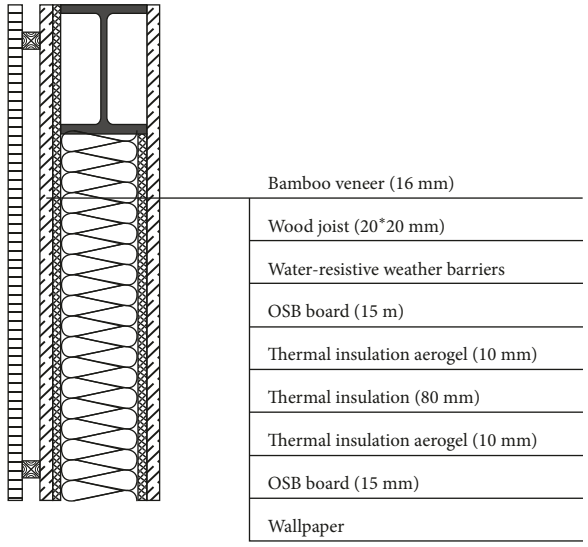

Figure 8: Construction design detail of an exterior wall using AB as the insulation material (source: authors' own data).

Figure 9: Full-scale model (source: authors' own data).

building's envelope and also to prevent natural creatures near the ground from entering into the building through the hole. The middle of the outer layer, 60 degrees up and down to a height of 1.7 m, was considered the sight zone, with larger holes to ensure users have an adequate view. The southern facade also needed to consider shading during the summer. Therefore, the hole size was reduced at the upper part of the interface, which prevented excessive solar radiation from entering.

The climate adaptation design is also embodied in the opening mode of the DSF interface. The outer interface could turn from 0 to 90 degrees by using an intermediate axis (as shown in Figure 13). In addition, in order to maximize the flexibility of the usage mode, the detailed design combined a middle axis rotating shaft together with a horizontal push-and-pull rail. Thus, the standard-sized outer interface could be completely retracted at both the western and eastern ends of the building in order to provide an unshielded view or multiple interface forms (as shown in Figure 14).

Important aspects of prefabricated buildings are the standardization and modularization of their design [36]. Besides the outer layer of the DSF, this design tested in this research was also based on the building components' standardization with multiple functions in order to realize various approaches to climate responsibility and adaptability. To achieve goals such as sight penetration and occlusion, natural lighting, shading, thermal insulation, preheating, ventilation, air filtration, the provision of natural risk barriers, sound insulation, and climate buffering, five basic facade treatments were designed: perforated aluminum plates, glass panels, air filter membranes, mosquito net panels, and AB insulation panels. The five interfaces formed a dynamic building interface with different functions that replaced more climate-orientated arrangements (as shown in Table 1). Each interface module was designed to fit the same component size, could be prefabricated as standardized in the factory, and was installed on the metal frame. There were also three trough-cable rails that could be inserted into the metal frame. With a single-slice, double-layer, or three-layer combination arrangement, users could set up these prefabricated interface modules according to their requirements, ultimately achieving a higher building environment performance (as shown in Figure 15).

3. Results and Discussion

3.1. Thermal Environment Performance Evaluation of the Integrated Building Envelope

3.1.1. Comprehensive Thermal Performance of the Integrated Building Envelope. The heat transfer coefficient of a material characterizes its heat transfer capacity, and the comprehensive heat transfer coefficient of a wall indicates the

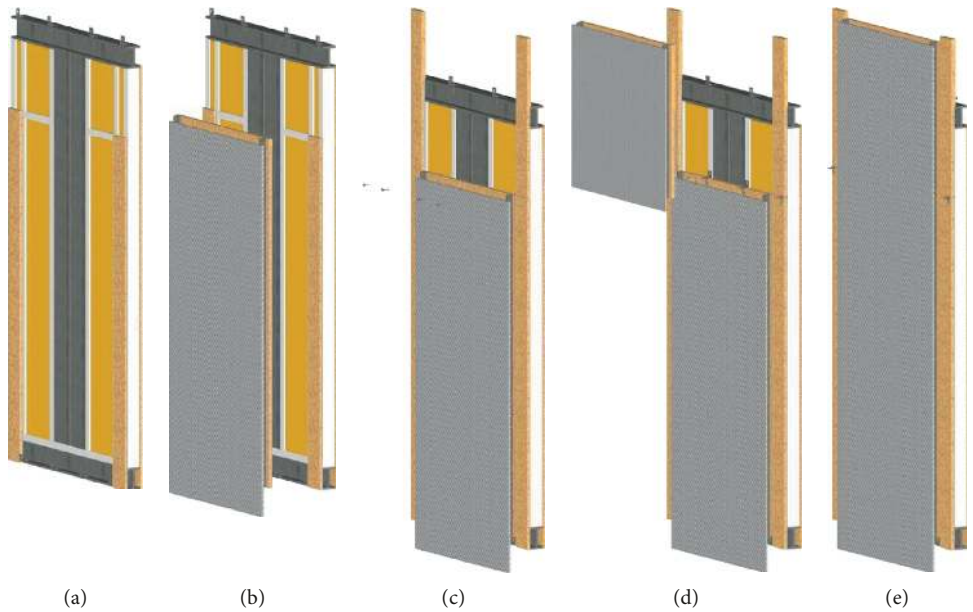

Figure 10: Installation instructions for an integrated building envelope using AB (source: authors' own data). (a) The foundation wall at the junction of two modules; (b) integrated wall including exterior decoration, heat preservation, and structural plates; (c) fix integrated wallboard by self-tapping pin; (d) install the upper (parapet) wall; (e) finish.

Figure 11: Full-scale model and connection details (source: authors' own data).

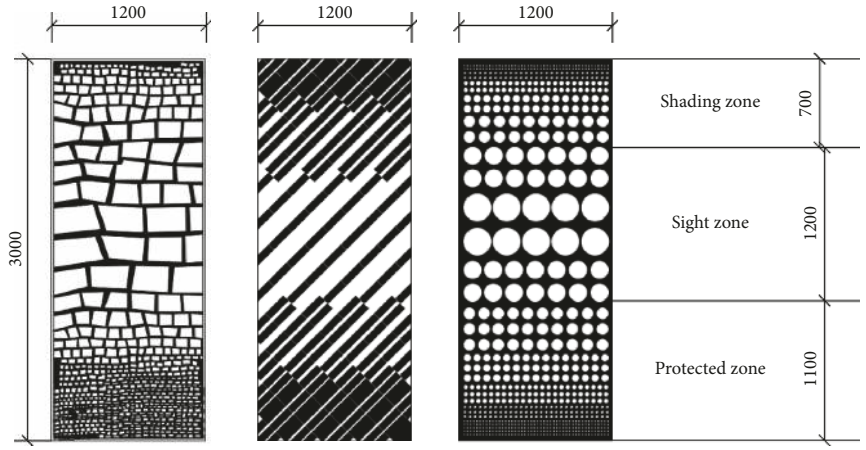

Figure 12: Vertical division of the sample outer layer (source: authors' own data).

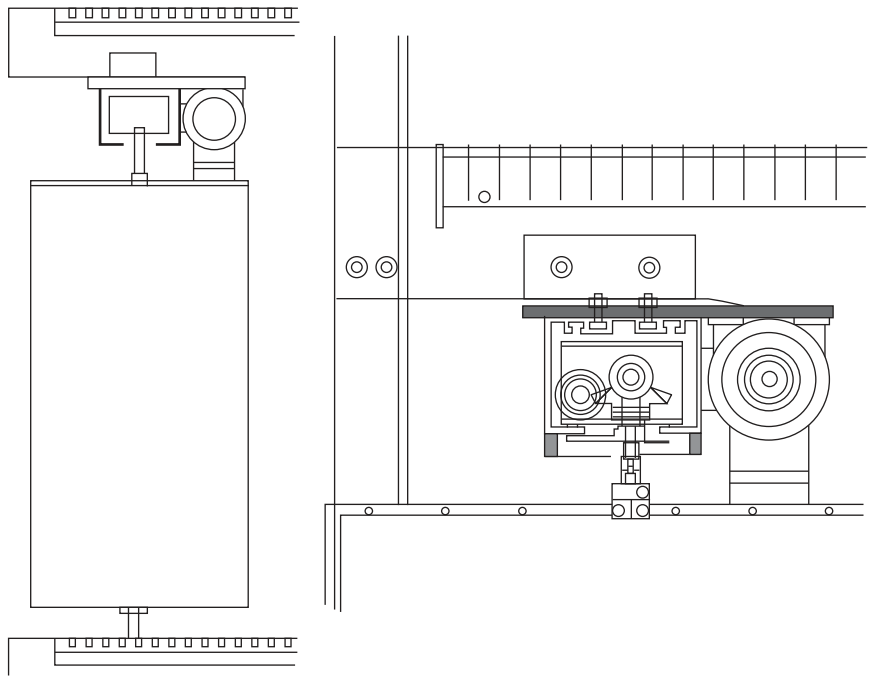

Figure 13: Detailed design of a combined middle axis rotating shaft and horizontal push-and-pull rail (source: authors' own data).

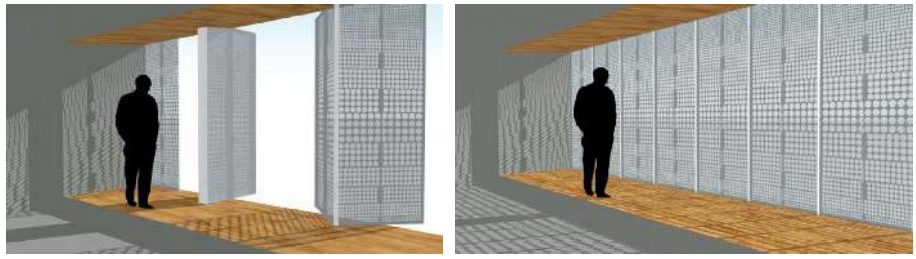

Figure 14: A combined middle axis rotating shaft and horizontal push-and-pull rail to realize multiple interface forms (source: authors' own data).

thermal insulation performance of a building. According to the official Chinese standard in the *Design Standard for Energy Efficiency of Public Buildings*, if a building's shape coefficient is less than 0.30, the heat transfer coefficient of the exterior wall should be no higher than 0.50 W/(m^2·K). If a building's shape coefficient is between 0.30 and 0.50, the heat transfer coefficient of the exterior wall should be no higher than 0.45 W/(m^2·K) in cold climate zones [37]. If a building's shape coefficient is less than 0.30, the heat transfer coefficient of the building's roof should be no higher than 0.45 W/(m^2·K). If the building's shape coefficient is between 0.30 and 0.50, the heat transfer coefficient of the building's roof should be no higher than 0.40 W/(m^2·K) in cold climate zones [37]. The comprehensive heat transfer coefficient achieved by using two kinds of thermal insulation is shown in Table 2. As compared to the national standard, the heat transfer coefficient achieved when using HIPs as the insulation material was calculated as saving 73%~76%. The heat transfer coefficient achieved by using ABs as the thermal insulation material was 43%~49%, as compared to the national standard.

The equation for calculating the comprehensive heat transfer coefficient of a building's exterior (nontranslucent) envelope is shown here as (1). Therefore, the comprehensive heat transfer coefficient, K_0, of the external walls and roofs, based on the two kinds of thermal insulation materials, can be calculated as shown in Table 2:

$$K_0 = \frac{1}{\sum R_0} = \frac{1}{R_i + R_n + R_e} = \frac{1}{R_i + (\delta_1/\lambda_1) + (\delta_2/\lambda_2) + (\delta_3/\lambda_3) + \cdots + (\delta_n/\lambda_n) + R_e}, \quad (1)$$

where R_i is the heat transfer resistance value of the inner surface. According to the shape relation of the building and climate conditions, the value can be obtained as 0.11 m^2·K/W. The variable R_n represents the comprehensive heat transfer resistance of the wall, and R_e is the heat transfer resistance value of the outer surface. According to the surface features of the building and the climatic conditions, the value can be obtained as 0.05 m^2·K/W. The variable

Table 1: Dynamic combinations of replaceable interface modules.

Layer	Number	Component	Function
Single slice	1	Perforated aluminum plate	Building facade, sun shading, natural risk barrier, sight penetration, and sight occlusion
	2	Glass panel	Buffer layer forming a double curtain wall to preheat the indoor space during winter
	3	Mosquito net panel	Insect barrier and ventilation
Double layer	4	Perforated aluminum plate + mosquito net panel	Building facade, sun shading, insect barrier, sight penetration, sight occlusion, and ventilation
	5	Perforated aluminum plate + air filter membrane	Building facade, sun shading, natural risk barrier, sight penetration, sight occlusion, and air purification
	6	Glass panel + mosquito net panel	Moderate ventilation and heat preservation during transition seasons
	7	Perforated aluminum plate + perforated aluminum plate	Composite interface to adjust building illumination
Triple layer	8	Perforated aluminum plate + AB insulation panel + perforated aluminum plate	A buffer layer to improve thermal insulation during winter nights
	9	Glass panel + mosquito net panel + air filter membrane	Sight penetration, moderate heat preservation, air filtration, and an insect barrier for transition seasons
	10	Perforated aluminum plate + AB insulation panel + glass panel	Integrated design of the building facade, sun shading, heat preservation, and preheating buffer zone
	11	Perforated aluminum plate + AB insulation panel + air filter membrane	Building facade, sun shading, heat preservation, and air filtration
	12	Glass panel + AB insulation panel + glass panel	Buffer layer, preheating, and heat preservation, suitable for winter and nighttime in cold climate zones

Source: authors' own data.

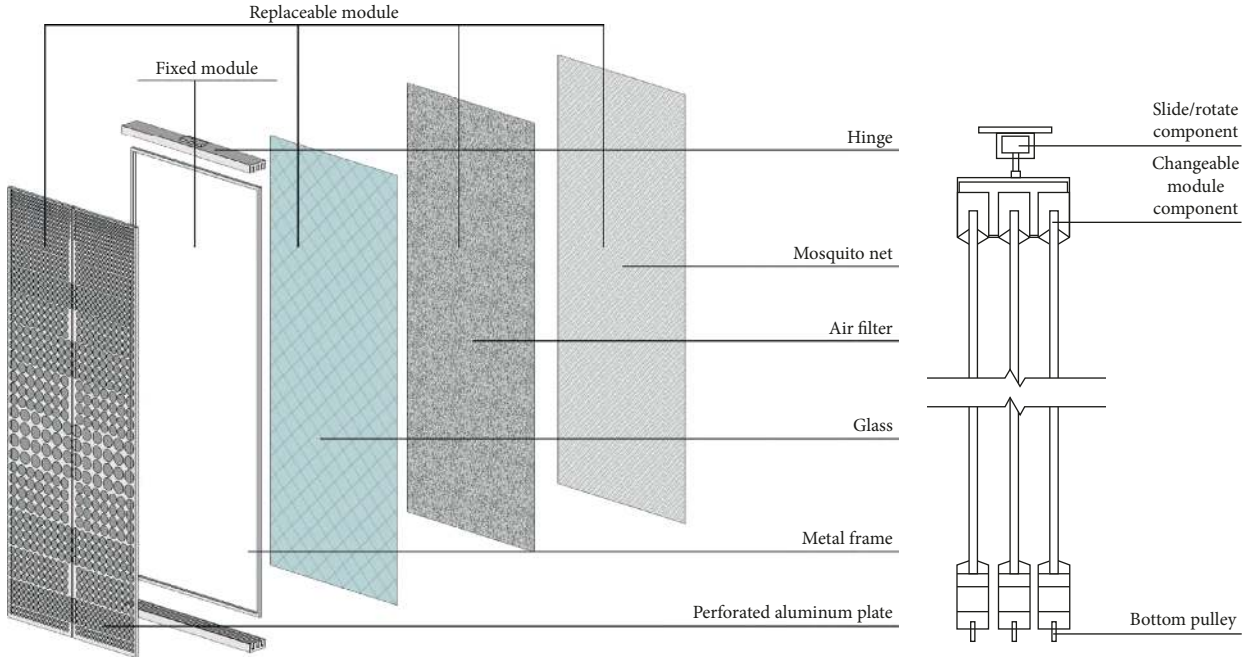

Figure 15: Replaceable modules based on climate adaptability (source: authors' own data).

δrepresents the thickness of the material (in mm), and λ is the material's thermal conductivity (in W/(m·K))

3.2. Evaluation of the Indoor thermal Environment

3.2.1. Experimental Setup and Measurement Conditions. The building used in this experiment was located in a cold climate zone in Beijing, China. It was a net-zero independent house that had adopted a modular prefabricated building system. The shape coefficient was 0.44, and the building construction footprint was 82 m^2 (as shown in Figure 5); HIPs were used as the insulation material (as shown in Table 2) [38]. To test the effectiveness of the insulation construction detail in different climate conditions over the course of an entire year, the test period was divided into four separate phases. Together, the four phases lasted more than

Table 2: Heat transfer performance of the integrated envelope.

Construction details of the integrated prefabricated building envelope	Position	Construction details (from interior to exterior)	Comprehensive heat transfer coefficient of the building's exterior (nontranslucent) envelope
Using HIPs as a thermal insulation material	Exterior wall	6 mm bamboo exterior finished surface; two 15 mm layers of HIP insulation; waterproof layer; 18 mm OSB structural board; light steel structural infill with 80 mm thick rock wool insulation panel; 9 mm interior finished surface	0.124 W/(m^2·K)
	Building roof	20 mm bamboo plywood surface layer; waterproofing membrane; 20 mm bamboo plywood surface layer; two 15 mm layers of HIP insulation; 18 mm OSB structural board; light steel structural infill with 140 mm thick rock wool insulation panel; 9 mm interior finished surface	0.105 W/(m^2·K)
Using ABs as a thermal insulation material	Exterior wall	12 mm aluminum plastic panel with air gap; 10 mm AB insulation; waterproof layer; 18 mm OSB structural board; light steel structural infill with 80 mm thick rock wool insulation panel; 6 mm AB insulation; 9 mm OSB interior finishing board	0.257 W/(m^2·K)
	Building roof	20 mm bamboo plywood surface layer; waterproofing membrane; 20 mm bamboo plywood surface layer; 10 mm AB insulation; 18 mm OSB structural board; light steel structural infill with 140 mm thick rock wool insulation panel; 6 mm AB insulation; 9 mm OSB interior finishing board	0.194 W/(m^2·K)

Source: authors' own data.

Table 3: Building information.

Climate zone	Cold climate zone in China
Build time	2013
Surrounding environment	In sculpture park, surrounded by green space
Building area	82 m^2
Building size	12.1 m (L) × 7.2 m (W) × 3 m (H)
Building storey	1 F
Building structure	Steel frame
Glazing size	South: 40 m^2; north: 7.8 m^2
Details and parameters	(i) Four layers of low-e insulating glass with a thickness of 5 mm/42 mm and a U-value of 0.48 W/(m^2·K), a shading coefficient of 0.443 for the south glazing wall
	(ii) Wall material: 80 mm mineral wool + HIP, a U-value of 0.2 W/(m^2·K)
	(iii) Roof material: 130 mm mineral wool and HIP, a U-value of 0.1 W/(m^2·K)
	(iv) PV system: 70 m^2 PV panels with a capacity of 11.5 kW, thin film photovoltaic panels
Other strategies	(v) Solar thermal: solar vacuum tube collectors
	(vi) HVAC: WSHP (cop = 6) and ASHP
	(vii) Water system: membrane bioreactor water treatment technology

Source: authors' own data.

one year, beginning in the December of 2013 and ending in the January of 2015. This research selected two physical quantities, temperature and heat flux, which were determined to reflect the thermal environment quality of the building. The goal was to test the actual thermal performance of the structure during the operating phase (Table 3) [39].

3.2.2. Results and Discussion. Figure 16 shows a comparison of the building's indoor and outdoor temperatures during winter, transition seasons, and summer. Through the temperature curve, it can be seen that the outdoor temperature fluctuated conspicuously in winter. During the test period, the highest temperature was 16°C and the lowest was −3.2°C. While the amplitude of the indoor temperature's fluctuation was very small, its actual fluctuation ranged ±3 degrees above or below 5°C. The indoor temperature was influenced very little by the external temperature, indicating the good insulation ability of the building (as shown in Figure 16(a)). During the transition season (spring), the highest outdoor temperature was 33.8°C and the lowest temperature was 6.7°C; the indoor temperature fluctuated within a range of ±6 degrees above or below 18°C (as shown in Figure 16(b)). In summer, the highest outdoor temperature was 50.3°C, while the lowest temperature was 14.1°C; this meant that the maximum temperature difference in the outdoors reached

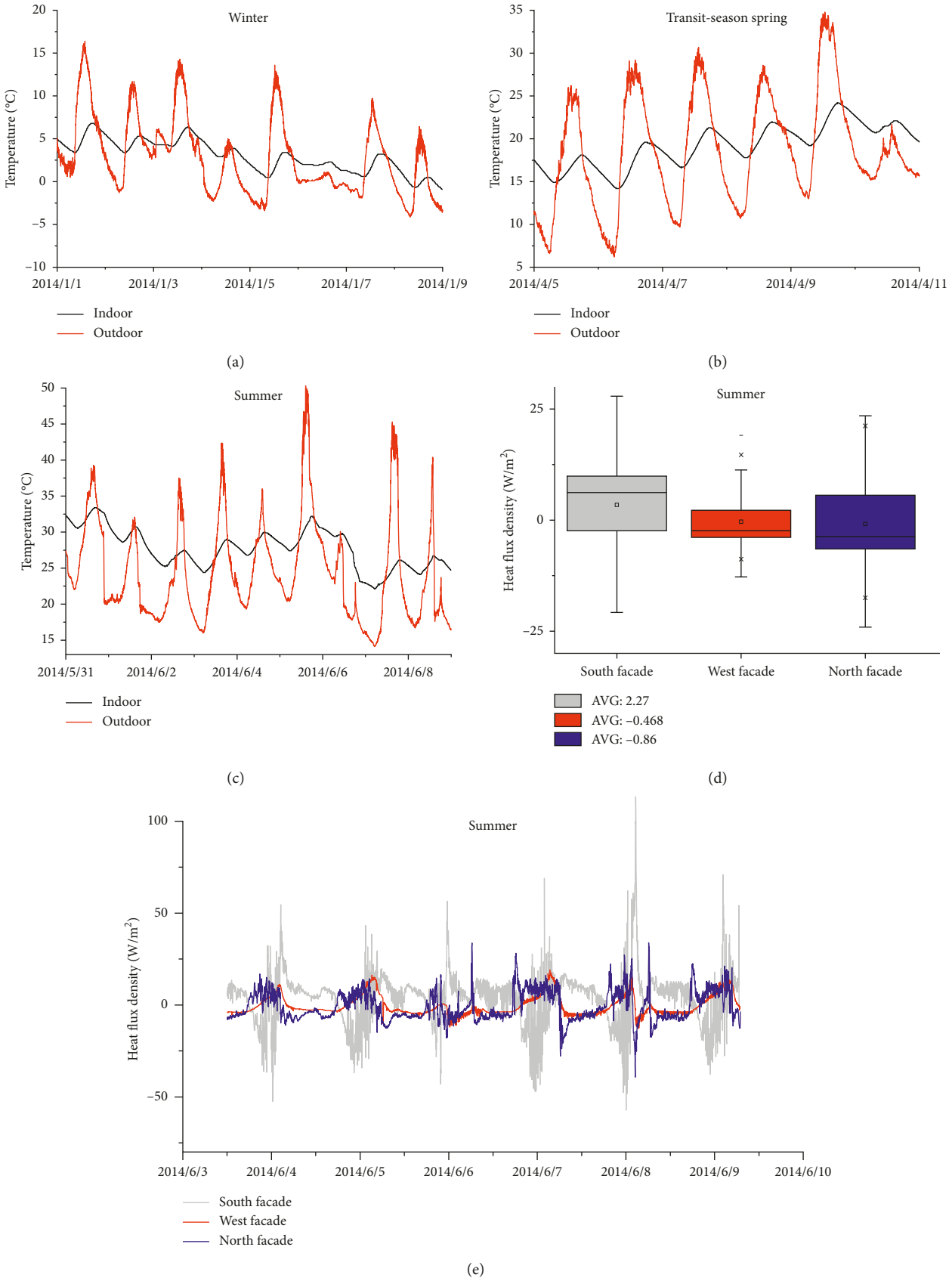

Figure 16: Thermal environment test of a modular prefabricated building using HIPs as the insulation material (source: authors' own data). (a) Winter temperatures; (b) transitional season temperatures; (c) summer temperatures; (d) floating box line diagram of summer heat flux density; (e) hourly curve diagram of summer heat flux density.

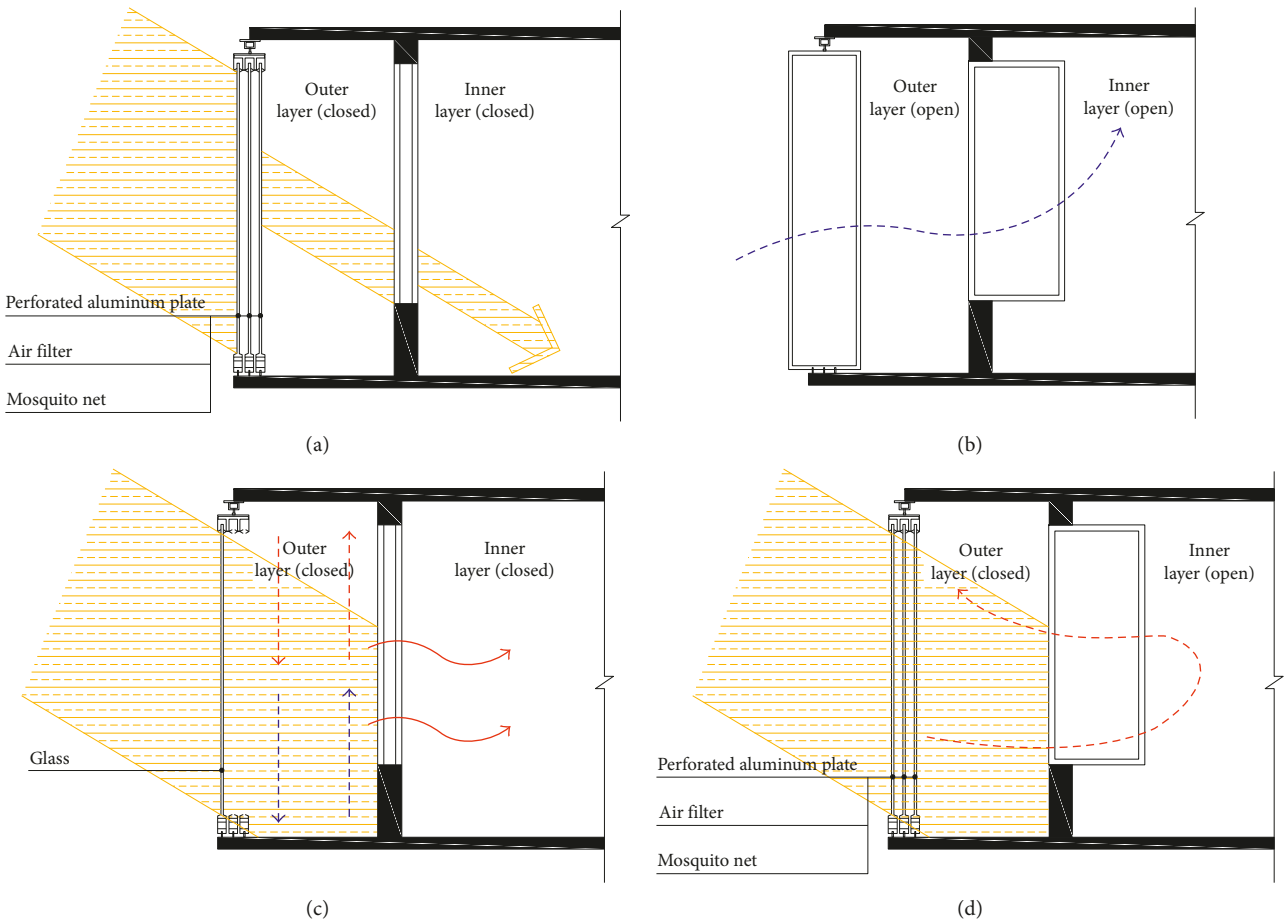

FIGURE 17: The climate adaptation mode of the integrated changeable modules throughout the building's entire life cycle (source: authors' own data). (a) Shading/air filter mode (summer day); (b) natural ventilation mode (summer night); (c) sunspace mode (winter day); (d) sunspace/air filter mode (spring and autumn days).

36.2°C, while the indoor temperature difference was only 8.5°C. This indicates the building's excellent thermal insulation performance (as shown in Figure 16(c)).

The curves in Figures 16(d) and 16(e) illustrate the heat flow densities for the test building's southern, western, and northern walls during summer weather conditions. As can be seen in Figure 16(d), although the southern facade absorbed a considerable amount of solar radiation, the difference among the average heat flux densities for the three facades was very little: southern facade (2.27 W/m^2) > northern facade > (0.86 W/m^2) > western facade (0.48 W/m^2). Therefore, the overall heat gain was relatively small. Figure 16(e) illustrates the changes in the hourly heat flux density curve and thus the differences among the three facades. The fluctuation was more obvious in the southern facade than in the northern and western facades, due to the influence of summer solar radiation.

3.3. The Climate Adaptability of an Integrated Structure throughout an Entire Life Cycle. Section 2.2 addressed an integrated changeable module facade based on a DSF. Combining the different open and closed status modes of the inner and outer layers simulated the usage pattern of the building throughout an entire year's climatic conditions. Figure 17 illustrates the four modes and all statuses, including the shading/air filter mode in the summer during the day, natural ventilation mode in the summer at night, sunspace mode in winter during the day, and sunspace/air filter mode during the transition season. The simulation of thermal conditions focused on the typical climatic week of an entire summer day and an entire winter day. The comparisons of indoor and outdoor temperatures and cooling and heating loads before and after changes in the variable interface are discussed below.

During summer days, the interface was used to block excess sunlight. The result was that the outer interface of the changeable DSF facade had three layers of modules, including (from outside to inside) a perforated aluminum plate, an air filter, and a mosquito net, all of which played a role in shading and air filtration. Figure 18 shows the thermal environment data for the perforated aluminum plate shading in the experimental building (the building used in this experiment is shown in Figure 5. The shape of the building was rectangular. The size ratio was 12 m (L) × 5.7 m (W) × 3 m (H). The DSF facade was located on the

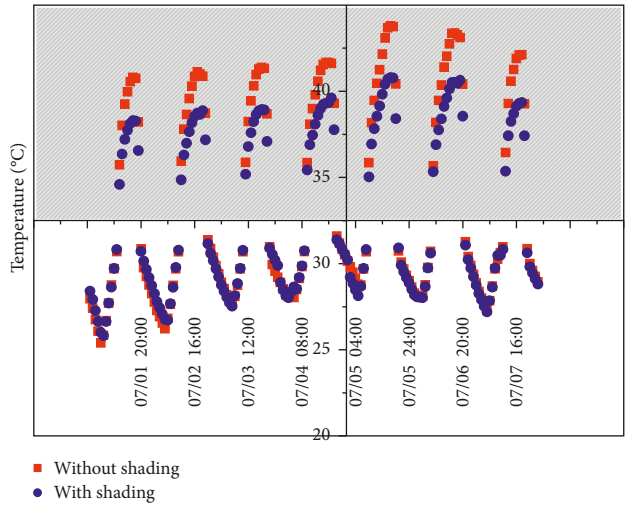

Figure 18: Temperature comparison with and without shading/air filtration mode (source: authors' own data).

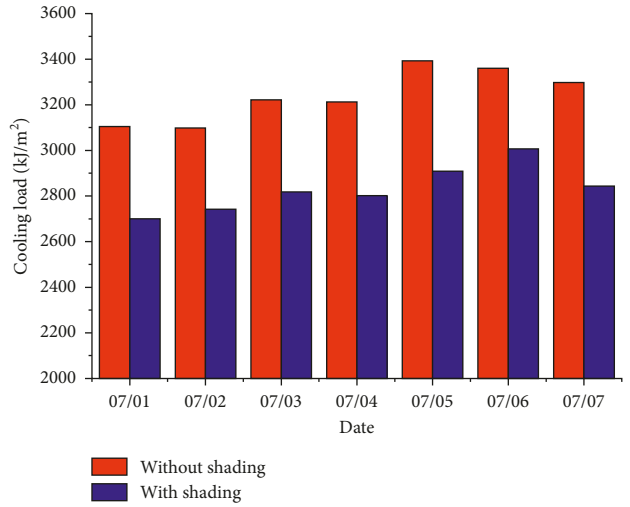

Figure 19: Cooling load comparison with and without shading/air filtration mode (source: authors' own data).

southern facade of the building) in the hot summer and warm winter zones of Shenzhen, during a typical work week (from July 1 to July 7). The red curve indicates the interior temperature environment without shading, and the blue curve illustrates the interior temperature when the sun shading board was in use. This clearly illustrates that the sun-shaded plate inhibited heat transfer, especially during high-temperature times (over 35°C). The maximum temperature difference with and without sun shading was 3°C. Figure 19 shows the corresponding cooling load histogram, which shows that the cooling energy load saving was 10.5%~14.2% from 7 am to 6 pm.

During winter days, the greenhouse effect in the sunspace will preheat the indoor space, improving the indoor temperature and reducing the energy consumption demand. Therefore, a single layer of glass or ETFE film was inserted into the outer interface of the DSF; its effect is shown in Figure 20. This research simulated the combined glass interface and corridor of the experimental building, which were used as a sunspace. The building was located in a cold area, Beijing, during a typical work week (from January 1 to January 7). The red curve illustrates the interior temperature environment without the glass interface, and the blue curve indicates the interior temperature with the combined glass interface and corridor. Under the DSF preheating function, the indoor temperature improved throughout the day and had a positive effect on the indoor thermal environment. Especially during the daytime when there was ample solar radiation, the DSF mode was able to raise the indoor temperature by 2°C, and the highest temperature difference between the interior and exterior reached 5.7°C. Figure 21 shows the corresponding heating load in winter. Depending on the daily solar radiation, there was a marked difference in solar gain in the sunspace. Under typical conditions, this design mode saved heating energy consumption, on average, by approximately 24.6%; at its highest point, these savings reached 38.3% during the daytime, from 7 am to 6 pm, which obviously underscores the usefulness of preheating.

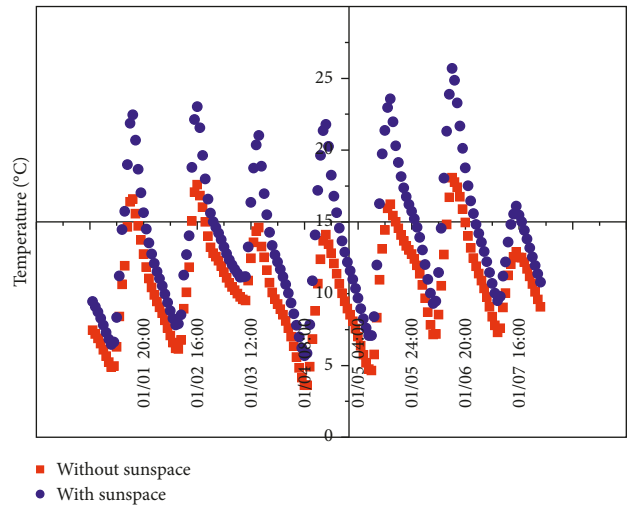

Figure 20: Temperature comparison with and without sunspace mode (source: authors' own data).

4. Conclusions

This research designed and evaluated a modular prefabricated building in an effort to improve its performance in terms of sustainability. Certain prefabricated construction details of the modular building envelope were studied, beginning with the steel frame of the modular structural system. In order to improve construction efficiency in this type of modular prefabricated building, as well as to enhance the physical environment and reduce energy consumption during the operational phase via integrated thermal insulation, two basic prefabricated envelope units were developed. The first employed high-performance thermal insulation materials to produce an integrated building envelope and modular connection points, the goal of which was to improve the building's performance in terms of sustainability. The second used the DSF principle to study how changeable module envelope units respond in terms of

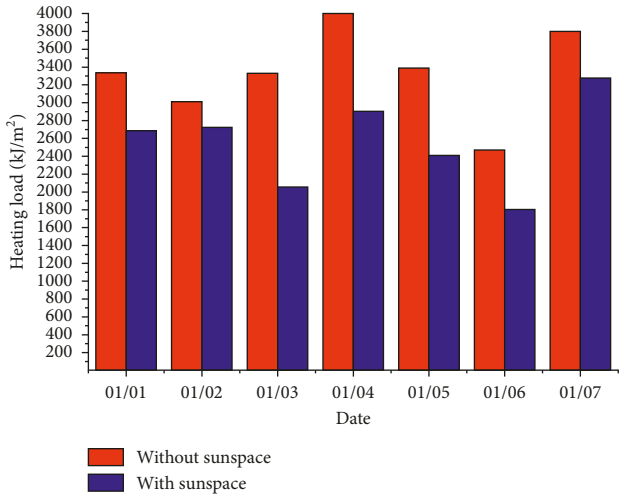

Figure 21: Heating load comparison with and without sunspace mode (source: authors' own data).

climate adaptability. By constructing an experimental building, full-scale model, and computer simulation, this research verified the feasibility and effectiveness of several integrated building envelope units. This research has contributed to the literature in three key ways:

(1) This study selected two types of thermal insulation materials, high insulation panels and aerogel blankets, in order to study certain construction details of integrated building envelopes in modular prefabricated buildings. The comprehensive heat transfer coefficients for the two integrated envelopes were 0.124 W/(m^2·K) and 0.257 W/(m^2·K). With energy savings of 75% and 45%, respectively, both offered insulation capacities significantly better than the current national standard.

(2) Focusing on the weakest heat point, the thermal bridge that occurs at modular connection points, this study attempted to use construction detail design and research to build an experimental building and full-scale building model. The goal was to explore and verify the feasibility of the climate-responsive construction technique called "reverse install." Long-term monitoring of the physical environment proved the effect of the integrated envelope on the connection points of two modules comprising a prefabricated building. When the outdoor temperature difference reached 36.2°C during summer days, the interior temperature difference was only 8.5°C. This illustrates the excellent thermal insulation performance of the building envelope's design.

(3) To address issues related to climate change, building facade units were dynamically adjusted via different modular building envelope units; these included sunshades, preheaters, ventilation, air filtration, pest control, and other functional elements designed to improve the building's climate adaptability performance. The effects of the changeable building envelope units were verified by the computer simulation. Sun shading in Shenzhen was shown to save cooling energy load consumption by 10.5%~14.2% during the daytime; similarly, in Beijing, sunspace was shown to save the average daily heating load consumption by approximately 24.6%.

Data Availability

The data used to support the findings of this study are available from the corresponding author upon request.

Conflicts of Interest

The authors declare that they have no conflicts of interest.

Acknowledgments

This work was supported by the Fundamental Funds for China Postdoctoral Science Foundation Funded Project (Project no. 2017T100035) and the National Natural Science Foundation of China (Grant nos. 51708019 and 51678324).

References

[1] H. Lin, "The design and analysis of sustainable architecture system," *Architecture Journal*, vol. 12, pp. 15–17, 2003.

[2] O. Oduyemi and M. Okoroh, "Building performance modelling for sustainable building design," *International Journal of Sustainable Built Environment*, vol. 5, no. 2, pp. 461–469, 2016.

[3] L. Caneparo, *Digital Fabrication in Architecture, Engineering and Construction*, Springer, Dordrecht, Netherlands, 2014.

[4] Y. Wang, L. Wang, E. Long, and S. Deng, "An experimental study on the indoor thermal environment in prefabricated houses in the subtropics," *Energy and Buildings*, vol. 127, pp. 529–539, 2016.

[5] G. Tumminia, F. Guarino, S. Longo et al., "Life cycle energy performances of a Net Zero energy prefabricated building in Sicily," *Energy Procedia*, vol. 140, pp. 486–494, 2017.

[6] Y. Teng, K. Li, W. Pan, and T. Ng, "Reducing building life cycle carbon emissions through prefabrication: evidence from and gaps in empirical studies," *Building and Environment*, vol. 132, pp. 125–136, 2018.

[7] E. Bonamente, M. C. Merico, S. Rinaldi et al., "Environmental impact of industrial prefabricated buildings: carbon and energy footprint analysis based on an LCA approach," *Energy Procedia*, vol. 61, pp. 2841–2844, 2014.

[8] M. Sonego, M. E. S. Echeveste, and H. G. Debarba, "The role of modularity in sustainable design: a systematic review," *Journal of Cleaner Production*, vol. 176, pp. 196–209, 2018.

[9] K. Salonitis, "Modular design for increasing assembly automation," *CIRP Annals*, vol. 63, no. 1, pp. 189–192, 2014.

[10] H. Zhang, J. Li, L. Dong, and H. Chen, "Integration of sustainability in Net-zero House: experiences in Solar Decathlon China," *Energy Procedia*, vol. 57, pp. 1931–1940, 2013.

[11] Z. Chen, J. Liu, Y. Yu, C. Zhou, and R. Yan, "Experimental study of an innovative modular steel building connection," *Journal of Constructional Steel Research*, vol. 139, pp. 69–82, 2017.

[12] G. Juanli, *Research on the Integration Performance of Industrialized Building Envelop Components of Affordable Housing in the Severe Cold Zone of China*, Tianjin University, Tianjin, China, 2013.

[13] N. Soares, P. Santos, H. Gervásio, J. J. Costa, and L. Simões da Silva, "Energy efficiency and thermal performance of lightweight steel-framed (LSF) construction: a review," *Renewable and Sustainable Energy Reviews*, vol. 78, pp. 194–209, 2017.

[14] H. Sozer, "Improving energy efficiency through the design of the building envelope," *Building and Environment*, vol. 45, no. 12, pp. 2581–2593, 2010.

[15] W. Boesiger and H. Girsberger, *Le Corbusier-euvre Complete*, Vol. 5, Birkhäuser, Basel, Switzerland, 1998.

[16] J. N. Habraken, *Conversations with Form: A Workbook for Students of Architecture*, Routledge, London, UK, 2014.

[17] Y. Yinjun, L. Dong Wei, and X. Lei, "The development and application of integration technology and industrial interior design in SI residential," *Architecture Journal*, vol. 4, pp. 55–59, 2012.

[18] Z. H. Jingxiang, "System or individuality–the wooden houses of Konrad Wachsmann and Frank Lloyd Wright in the 1930s," *Architecture Journal*, vol. 7, pp. 22–27, 2015.

[19] L. Caneparo, *Digital Fabrication in Architecture, Engineering and Construction*, Springer, Dordrecht, Netherlands, 2014.

[20] F. Ochs, D. Siegele, G. Dermentzis, and W. Feist, "Prefabricated timber frame façade with integrated active components for minimal invasive renovations," *Energy Procedia*, vol. 78, pp. 61–66, 2015.

[21] T. Konstantinou and U. Knaack, "An approach to integrate energy efficiency upgrade into refurbishment design process, applied in two case-study buildings in Northern European climate," *Energy and Buildings*, vol. 59, no. 4, pp. 301–309, 2013.

[22] Z. Li, M. He, X. Wang, and M. Li, "Seismic performance assessment of steel frame infilled with prefabricated wood shear walls," *Journal of Constructional Steel Research*, vol. 140, pp. 62–73, 2018.

[23] J.-H. Song, J.-H. Lim, and S.-Y. Song, "Evaluation of alternatives for reducing thermal bridges in metal panel curtain wall systems," *Energy and Buildings*, vol. 127, pp. 138–158, 2016.

[24] L. Zhenghao, S. Yehao, S. Jingfen et al., "Climate responsive modular building skin design strategy:a case study of the-studio," *Eco-City and Green Building*, vol. 2, pp. 54–61, 2015.

[25] R. Baetensa, B. P. Jellea, J. V. Thueb et al., "Vacuum insulation panels for building applications: a review and beyond," *Energy and Buildings*, vol. 42, no. 2, pp. 147–172, 2010.

[26] http://jxjc88.cn.china.cn/.

[27] L. Junjie, Z. H. Hong, Z. H. Yuting, and M. Jiajian, "Building envelop technology strategies in green building practices and its problems," *Eco-City and Green Building*, vol. 1, pp. 19–24, 2014.

[28] I. Smirnova and P. Gurikov, "Aerogel production: current status, research directions, and future opportunities," *Journal of Supercritical Fluids*, vol. 134, pp. 228–233.

[29] U. Berardi, "Aerogel-enhanced systems for building energy retrofits: insights from a case study," *Energy and Buildings*, vol. 159, pp. 370–381, 2018.

[30] K.-J. Lee, Y.-J. Choe, Y. H. Kim, J. K. Lee, and H.-J. Hwang, "Fabrication of silica aerogel composite blankets from an aqueous silica aerogel slurry," *Ceramics International*, vol. 44, no. 2, pp. 2204–2208, 2018.

[31] *The Brochure of Tianjin Langhua Science and Technology Development Co., Ltd.*, 2017, http://www.tjhykj.com/.

[32] Master Series, *The Works and Ideas of Herzog and Meuron–The Editing Department of the Master Series Books*, China Electric Power Press, China, 2004.

[33] S. Yehao, W. Jialiang, L. Caldas et al., "Indoor comfort and energy saving building performance created by envelop materials," *Time and Architecture*, vol. 3, pp. 77–81, 2014.

[34] Z. Su, X. Li, and F. Xue, "Double-skin façade optimization design for different climate zones in China," *Solar Energy*, vol. 155, pp. 281–290, 2017.

[35] S. B. Sadineni, S. Madala, and R. F. Boehm, "Passive building energy savings: a review of building envelope components," *Renewable and Sustainable Energy Reviews*, vol. 15, no. 8, pp. 3617–3631, 2011.

[36] P. Pihelo, T. Kalamees, and K. Kuusk, "nZEB renovation with prefabricated modular panels," *Energy Procedia*, vol. 132, pp. 1006–1011, 2017.

[37] Chinese National Standard, *Design Standard for Energy Efficiency of Public Buildings, GB50189*, Chinese National Standard, Taiwan, China, 2015.

[38] J. Li, Y. Song, and Q. Wang, "Experimental verification and pair-group analysis study of passive space design strategies," in *Proceeding of the 4th International Conference on Civil, Architecture and Hydrauic Engineering (ICCAHE'2015)*, Guangzhou, China, December 2015.

[39] S. Yehao, L. Junjie, W. Jialiang et al., "Multi-criteria approach to passive space design in buildings: impact of courtyard spaces on public buildings in cold climates," *Building and Environment*, vol. 89, pp. 295–307, 2015.

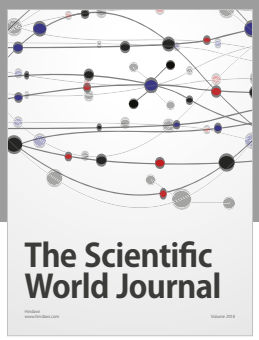

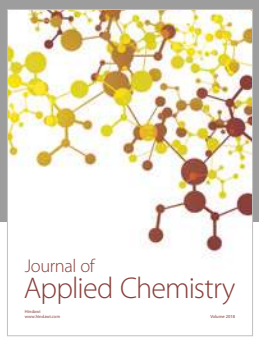

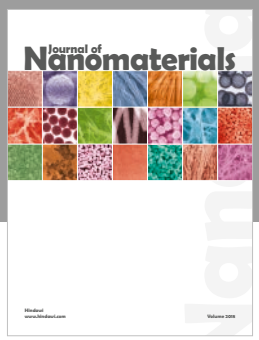

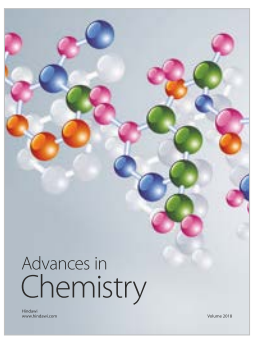

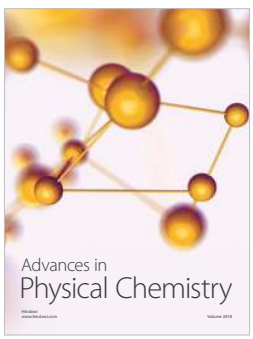

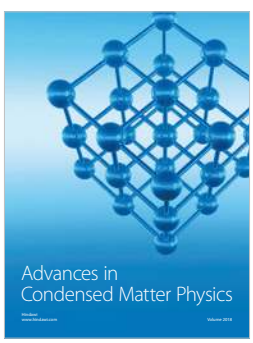

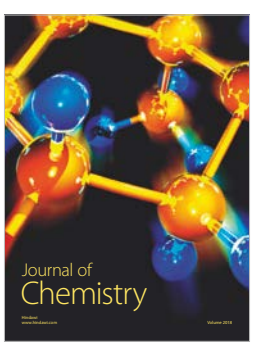

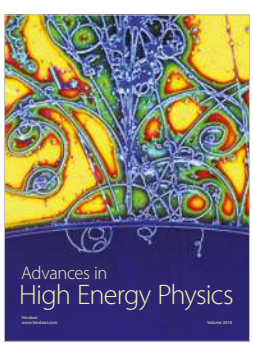

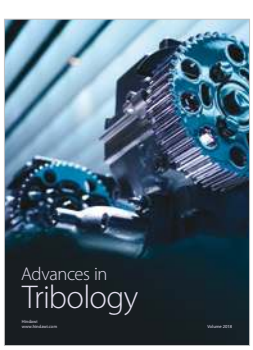

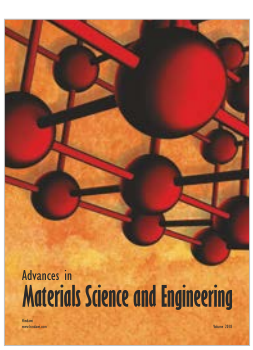

Hindawi

Submit your manuscripts at
www.hindawi.com